PerTPV – Perovskite thin film photovoltaics

Grant agreement 763977

Deliverable 4.3

Perovskite environmental fate studies

WP4

Lead beneficiary: FHNW
Authors: Felix Schmidt, Markus Lenz
Delivery date: 31/3/2021
Confidentiality level: Public

The PerTPV project has received funding from the European Union's Horizon 2020 research and innovation programme under grant agreement No 763977.

Revision History

Author Name, Partner short name	Description	Date
Felix Schmidt, FHNW	Draft deliverable	11/02/2021
Markus Lenz, Felix Schmidt (FHNW)	Revision 1	09/03/2021
Markus Lenz, Felix Schmidt (FHNW)	Draft deliverable	18/03/2021
Henry Snaith (UOXF)	Revision 2	30/03/2021

Contents

The PerTPV project has received funding from the European Union's Horizon 2020 research and innovation programme under grant agreement No 763977.

List of abbreviations

BCP – bathocuproine

FTO – fluorine-doped tin oxide

GC-MS – gas chromatography-mass spectrometry

(qqq) ICP-MS – (triple quadrupole) inductively coupled plasma mass spectrometry

ITO – indium tin oxide

LCF – linear combination fitting

PCBM – phenyl-C_{61}-butyric acid methyl ester

PEC – predicted environmental concentration

PEDOT:PSS – poly(3,4-ethylenedioxythiophene) polystyrene sulfonate

Poly-TPD – poly(4-butyltriphenylamine)

PSC – perovskite solar cell

Spiro-OMeTAD – 2,2',7,7'-Tetrakis[N,N-di(4-methoxyphenyl)amino]-9,9'-spirobifluorene

UOXF – University of Oxford

US EPA – United States environmental protection agency

VTT – Valtion Teknillinen Tutkimuskeskus, Technical research center of Finland

XAFS – X-ray absorption fine structure

XANES – X-ray absorption near edge structure

The PerTPV project has received funding from the European Union's Horizon 2020 research and innovation programme under grant agreement No 763977.

Abstract

Despite concerns regarding the possible negative impact of perovskite solar cells (PSC) in the environment (stemming from the presence of lead), studies on their environmental fate are still rare. Some studies claim that the impacts may be negligible due to the low Pb concentrations contained in PSCs. However, questions remain on how fast Pb is leaching from different PSCs and how bioavailable Pb will be in different (biogeochemical) conditions. Further, it is not yet clear how environmental concentrations can be predicted and how accurate and precise these predictions are. Therefore, a number of systematic fate studies in complex environmental systems were performed.

Soil-water microcosms were set up to investigate environmental fate of PSCs (both Pb and Sn based) in a worst-case scenario, i.e. immediate and quantitative metal release to soils. Using state-of-the-art trace metal analytics and soil sequential extraction measurements, these experiments showed rapid and efficient removal of Pb and Sn from the aqueous phase under a suite of environmental conditions. Soil sequential extraction revealed that substantial amounts of Pb and Sn are stably sequestered in soils naturally. Synchrotron-based X-ray absorption fine structure (XAFS) measurements on the Pb-L edge showed that sorption of perovskite-based Pb^{2+} onto mineral surfaces was likely the underlying sequestration mechanism in soils, despite thermodynamic equilibrium modelling indicating Pb precipitation. Sn was rapidly removed from the aqueous phase, even faster in comparison to Pb, and a stronger immobilisation was observed. In summary, rapid sequestration of the majority of metals (Pb > 91 %; Sn > 94 %) within 24 h argue in favour of PSCs, whereas sorption as the main mechanism of sequestration questions the irreversibility of Pb immobilization.

Leaching kinetics in PSCs have typically been carried out under standardized test conditions consisting of an extraction fluid (typically water or mild acid) and a single endpoint (typically after 24 hours). Such tests, even though useful for approximate simulation, do not give time-resolved information and hence are limited in predictive power. Here, we established a novel analytical tool to address metal leaching from PSCs on a smaller scale (micro-damage) and with time-resolved data. The system is based on image analysis (to monitor perovskite degradation) and trace metal analytics (to monitor metal leaching). This could represent a basis for novel tools to follow new cell development.
An assessment of toxicity using bioluminescent bacteria revealed that Pb^{2+} alone and not other PSC constituents determined the toxicity of possible PSC leachates. A first-of-its-kind outdoor installation was constructed to assess metal leaching from PSCs under natural weather conditions and to verify predicted metal concentrations. After 10 months of exposure, only minute amounts of Pb were released and encapsulation proven to be the critical parameter to limit metal release. Further, even without proper encapsulation, the amount of Pb^{2+} released was not quantitative. Lastly, fully encapsulated PSC devices were shown to withstand hail impact testing (> 40 mm) without substantial Pb^{2+} release.

The PerTPV project has received funding from the European Union's Horizon 2020 research and innovation programme under grant agreement No 763977.

1. Introduction

Environmental impacts from perovskite solar cell (PSC) constituents can arise throughout the products lifecycle[1–3]. Damage during the use-phase may result in metal leaching to the environment (water, soil)[4,5]. Further, leaching may occur at the end-of-life when PSC are not collected and recycled.
Up to date, studies on the environmental fate of PSC components are often either purely based on predictions and / or too simplistic laboratory systems. Therefore, direct experimental assessment of metal fate in complex environmental systems were performed and are summarised in this deliverable (Figure 1). Moreover, a toxicity assay using bioluminescent bacteria was developed, validated and used to address potential mixture effects arising in complex PSCs. Tools were developed to quantify leaching in damaged PSC systematically and predict resulting concentrations of metals in the environment. Ultimately, an outdoor rooftop installation has been designed to quantify metal emission and verify predictions (Figure 1).

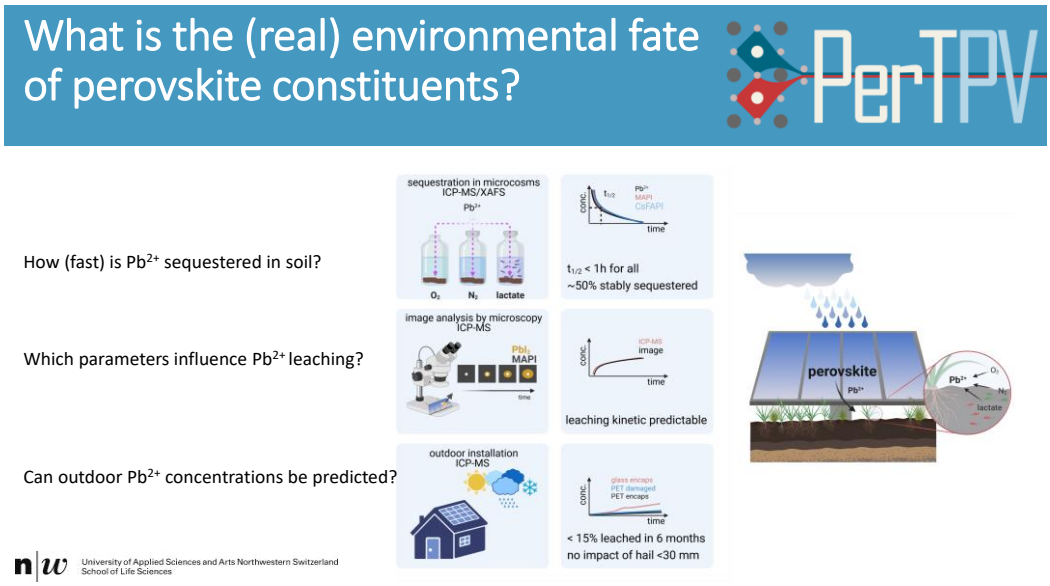

Figure 1: Overview of experiments to assess PSC environmental fate

2. Assessing Pb^{2+} fate in complex environmental systems

2.1 Soil-water microcosm experiments to assess fate

Microcosms were set up to simulate complex, environmental systems consisting of soil, rainwater and active microbes. The microcosms were tested under aerobic, anaerobic and lactate amended conditions to investigate metal partitioning in contrasting biogeochemical conditions (Figure 2). The microcosms were slurries of a loamy sand subsoil with low background Pb^{2+} concentration and a synthetic rainwater. Then, as a worst-case scenario, two sources of PSC Pb^{2+} ($MAPbI_3$ and $(FA_{0.83}Cs_{0.17})PbI_3$) were dissolved in rainwater and spiked into the systems, whereas a highly soluble lead salt ($Pb(NO_3)_2$) was used as control. Microbial activity in one set of microcosms was stimulated by addition of lactate.

The PerTPV project has received funding from the European Union's Horizon 2020 research and innovation programme under grant agreement No 763977.

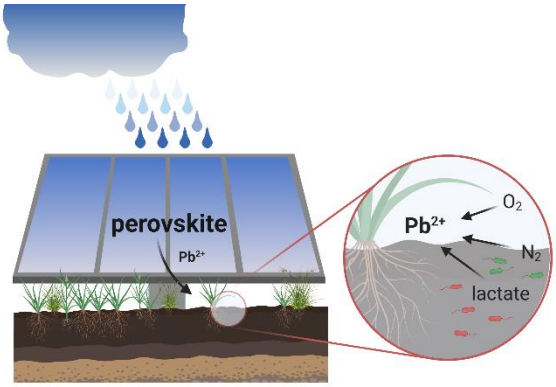

Figure 2: Schematic representation of soil-water-microcosm experiments simulating complex, environmental systems in aerobic and anaerobic conditions.

2.2 Removal of Pb^{2+} from the aqueous phase

Pb^{2+} concentration in the aqueous phase was monitored during the initial 24 h of the experiments via inductively coupled plasma mass-spectrometry (ICP-MS). MAPI, CsFAPI and $Pb(NO_3)_2$ species spiked in the soil-water systems showed fast and efficient removal from the aqueous phase in all conditions tested (data not shown, Figure 3 removed due to confidentiality). After 24 hours, the residual dissolved Pb^{2+} concentration was low and immediate (i.e. after 1 day) Pb^{2+} removal was between 91.4 and 97.6 %.

2.3 Irreversibility of Pb^{2+} sequestration

Pb^{2+} sequestration in microcosms was evaluated after 16 days of incubation by soil sequential extraction. For this, a sonication-assisted, accelerated sequential extraction procedure was carried out. Released Pb^{2+} was assessed after each step giving insight into possible mobility and / or bioavailability of Pb^{2+} in soils. One the one hand, Pb^{2+} extracted during the last two steps of the procedure can be considered irreversibly and stably sequestered, because they can be extracted only with harsh chemical extractants and elevated temperatures that are not environmentally relevant. On the other hand, Pb^{2+} from the first two steps can be considered possibly bioavailable.
In all tested conditions, a considerable fraction of Pb^{2+} was naturally immobilised and found in oxidizable and residual fractions and can thus be considered irreversibly sequestered (data not shown, Figure 4 removed due to confidentiality). Microcosms spiked with CsFAPI did not show a considerable difference in Pb^{2+} fractionation with redox conditions: About half (48.0 – 52.6 %) of spiked Pb^{2+} was irreversibly sequestered in oxidizable and residual fractions during the 16-day incubation, despite the conditions applied.
The remaining Pb^{2+} (i.e. extracted during the first two steps) may be mobilized in the environment and considered possibly bioavailable. Firstly, microbial activity can result in decreased soil pH by dissolution of CO_2 (as result of respiration)[6], by formation of sulfuric and nitric acid (result of microbial oxidation of ammonia and sulfide, formed from biomass degradation)[7,8] or by acidic rain[9]. Secondly, iron and manganese mineral phases can be reductively dissolved through microbes upon induction of reducing conditions (e.g. periodic flooding or heavy rain)[10,11]. Reducing conditions are known to occur even on short timescales (e.g. during water logging after rain or periodic flooding), possibly liberating Pb^{2+} in reducible fractions. Since a major proportion of Pb was found in possibly bioavailable fractions, the mechanism of sequestration was studied in further detail.

The PerTPV project has received funding from the European Union's Horizon 2020 research and innovation programme under grant agreement No 763977.

2.4 Insights into Pb^{2+} sequestration mechanism

Formation of oversaturated phases that may precipitate in the soil-water microcosm systems was modelled by thermodynamic equilibrium modelling based on i) soil composition, ii) rainwater constituents and iii) concentration of spiked species. Modelling indicated that, under the tested conditions (neutral pH, different redox states), pyromorphite (Pb phosphate mineral) precipitation was thermodynamically favoured. Thus, pyromorphite formation could represent the ultimate sink for Pb^{2+} removal in these systems. Sequential extraction can offer only insight into fractionation without direct information on Pb^{2+} speciation. Therefore, to assess solid-state speciation of Pb^{2+} in soil, Pb LIII-edge X-ray absorption near edge structure (XANES) spectroscopy experiments were performed at the superXAS beamline (Swiss Light Source, Villigen, Switzerland). Dried soil samples from the microcosms were measured and compared to a set of reference materials including i) starting material ii) likely precipitation products and iii) Pb^{2+}-sorbed mineral species. Sample spectra were fitted using linear combination fitting (LCF). The best fits obtained after LCF based on model compound spectra (Figure 5A) described the spectra well. LCF indicated the highest share of Pb^{2+} was present in a form similar to Pb^{2+} sorbed on solid phases in all samples (Table 1). Comparing the speciation results to the thermodynamic modelling shows that, based on XANES data, pyromorphite precipitation was kinetically limited and rapid sorption onto mineral phases was the key mechanism of Pb^{2+} sequestration.

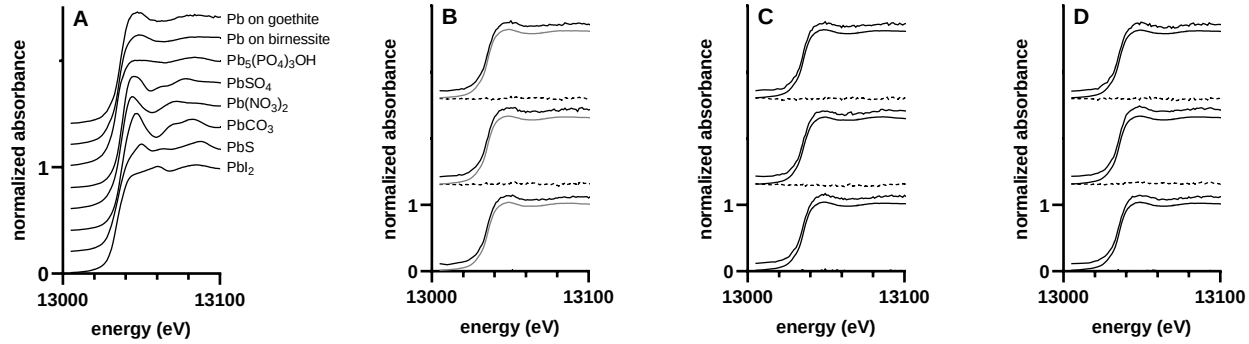

Figure 5: Normalized Pb LIII-edge XANES spectra for model compounds (A), MAPI (B), CsFAPI (C) and $Pb(NO_3)_2$) (D) derived Pb. Soil XANES spectra (B-D, solid lines) from aerobic (bottom), anaerobic (middle) and lactate amended (top) conditions are shown together with their best LCF fits (grey lines) and residuals from fits (dashed lines). Spectra are shifted in Y to improve readability.

For MAPI, most Pb^{2+} (100 %) of this species sorbed on solid phases was found in lactate amended microcosms, whereas for both CsFAPI and $Pb(NO_3)_2$, the highest share of such sorbed species was found in aerobic conditions (92 and 90 %, resp., Table 1). With one exception (18 % contribution of readily soluble species to anaerobic, CsFAPI-spiked microcosms, Table 1) only a minor fraction (<10 %) of Pb^{2+} was found as readily soluble species, indicating the majority was indeed stably sequestered in the soils (i.e. as sparingly soluble species or species sorbed on solid phases) in any condition.
During the sequential extraction procedure, birnessite is expected to be dissolved in the reducible fraction. The Pb mass balance during sequential extraction showed reducible fractions between 33 and 43 %, consistent with XAFS analysis. The remaining Pb in oxidizable and residual fractions are sorbed as well (indicated by LCF analysis), but likely on solids that are resistant to dissolution under reducing conditions. The formation of strong inner-sphere complexes of Pb in birnessite[12–14] would explain the difference

The PerTPV project has received funding from the European Union's Horizon 2020 research and innovation programme under grant agreement No 763977.

between sequential extraction and XAFS analysis. Hence, even though sorption might indicate potential release, they may still be considered irreversibly sequestered.

Table 1: Results of Pb Speciation modelled by Linear Combination Fitting of Pb LIII-Edge XANES Spectra (atom %)

Pb^{2+} species	solubility / condition	readily soluble species (%)	sparingly soluble species (%)	species sorbed on solid phase (%)
MAPI	aerobic	4	12	84
	anaerobic	0	15	85
	lactate amended	0	0	100
CsFAPI	aerobic	0	8	92
	anaerobic	18	20	61
	lactate amended	0	9	91
$Pb(NO_3)_2$	aerobic	0	10	90
	anaerobic	0	17	83
	lactate amended	9	3	88

2.5 Removal of Sn from the aqueous phase and irreversibility of sequestration

Soil-water microcosm experiments were also carried out for Sn-based perovskite precursors using the same setup as described in Section 2.1. Tin is considered the most likely substitute for Pb in PSCs[15,16]. However, efficiency and stability of Sn-based PSCs are still considerably lower when compared to their Pb-based counterparts. Here, $MASnI_3$ and $Sn(NO_3)_4$ were compared under aerobic and anaerobic conditions and monitored via aqueous Sn concentrations and soil sequential extraction (Figure 6).

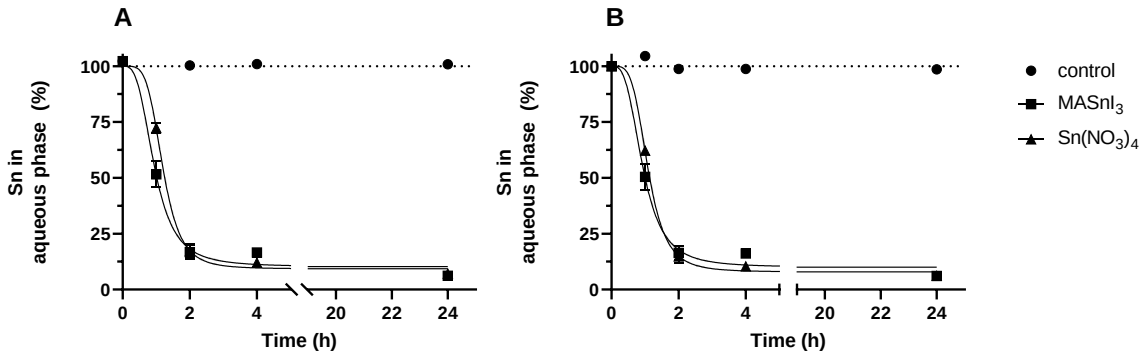

Figure 6: Monitoring of aqueous Sn concentrations over time for $MASnI_3$ and $Sn(NO_3)_4$ under aerobic (A) and anaerobic (B) conditions.

Sn removal from the aqueous phase followed a similar trend compared to Pb-based species. A short half-life (0.93-1.12 h) was observed for aerobic and anaerobic conditions (Figure 6 A,B). Total removal of Sn after 24 hours exceeded 94 % under all tested conditions. Soil sequential extraction did not show quantitative recovery (in contrast to Pb) still, there was hardly any possible bioavailable Sn (i.e. fractions “exchangeable” and

The PerTPV project has received funding from the European Union’s Horizon 2020 research and innovation programme under grant agreement No 763977.

"reducible"). The highest fraction of Sn was observed in the last step of the extraction. The relative amount of potentially mobile Sn was less than 2.5 % (data not shown).

2.6 Biotransformation of Sn-based PSCs

Unlike Pb, Sn species can be biotransformed to alkylated species. Organotin species are environmental contaminants well known for their endocrine disruptive nature[17,18], that negatively impacts ecosystems at extremely low concentrations. Therefore, an analytical method using gas chromatography-mass spectrometry (GC-MS) was developed to assess the formation of methylated tin species (Figure 7), even if sequential extraction showed most Sn stably sequestered. The method included derivatisation with $NaB(OEt)_4$ and detection limits were in the low µg/L range. This would allow detecting as little as 0.05-0.5 % of spiked Sn in microcosms.

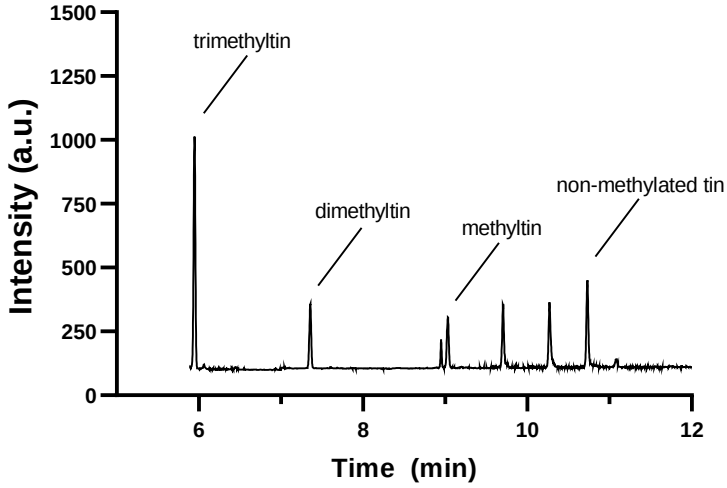

Figure 7: Separation of 4 tin species (Methyl-/Dimethyl-/Trimethyl-/ and non-methylated tin) by GC-MS (250 µg/L each; total ion count)

Samples from the microcosm reactors were tested for methyl tin species formation, but did not show any peaks under various conditions. Therefore, the formation of organotin species under the tested conditions is considered unlikely.

2.7 Toxicity of Pb and Sn-based PSCs

Generally, ionic Sn is less critical and toxic to environmental systems and human health[19]. Nonetheless, recent studies carried out indicated that toxicity of SnI_2 was in fact higher than that of PbI_2. The authors related this finding to a lower pH generated upon dissolution of SnI_2 and therefore suggested acidity as the main driver of toxicity, not the ionic metal[20].

To elucidate on Sn and Pb (mixed) toxicity, a toxicity assay was developed and validated based on bioluminescent bacteria (*Aliivibrio fischeri*). A recent study evaluated various species for their toxicity sensitivity and demonstrated that *Aliivibrio* fischeri, of the tested organisms, was the most sensitive[21]. Briefly, the bacteria were treated with a given test substance for 30 minutes as a simple endpoint assay. The inhibited bioluminescence was quantified and used to construct dose-response curves (Figure 8). Toxicity of PbI_2 and $MAPbI_3$ was compared and showed similar results as literature values[21]. Furthermore, a synthetic PSC solution was tested. The solution was based on a PSC

The PerTPV project has received funding from the European Union's Horizon 2020 research and innovation programme under grant agreement No 763977.

with Al / spiro-OMeTAD / $MAPbI_3$ / SnO_2 / ITO composition, where the chemicals were added in appropriate ratios into an aqueous solution. The maximal tested concentrations were based on aqueous Pb concentrations of 20 mg/L. This is identical to the aqueous concentration applied in microcosm experiments and therefore simulates a worst-case leaching scenario. The resulting dose-response curves did not differ significantly and therefore no mixture effects could be observed. Independent of other soluble PSC constituents, Pb^{2+} concentration determined the toxic effect on bioluminescent bacteria. Other perovskite precursor components (MAI, FAI, CsI, KI) were also tested, but did not show any significant bioluminescence inhibition in the tested concentration range. Sn-based species were tested as well. SnI_2 and $Sn(NO_3)_4$ did not lead to suitable dose-response curves in the tested concentration range. The bioluminescence assay, even though highly sensitive, has some limitations based on a lack of specificity. Subtle changes such as pH differences or changes on a cellular level cannot be seen. Therefore, PbI_2 toxicity in this assay was shown to be higher than SnI_2, in contrast to Babayigit et al. Further mixture toxicity assessment (e.g. on the role of iodide) with different organisms and endpoint are therefore required for a more complete picture.

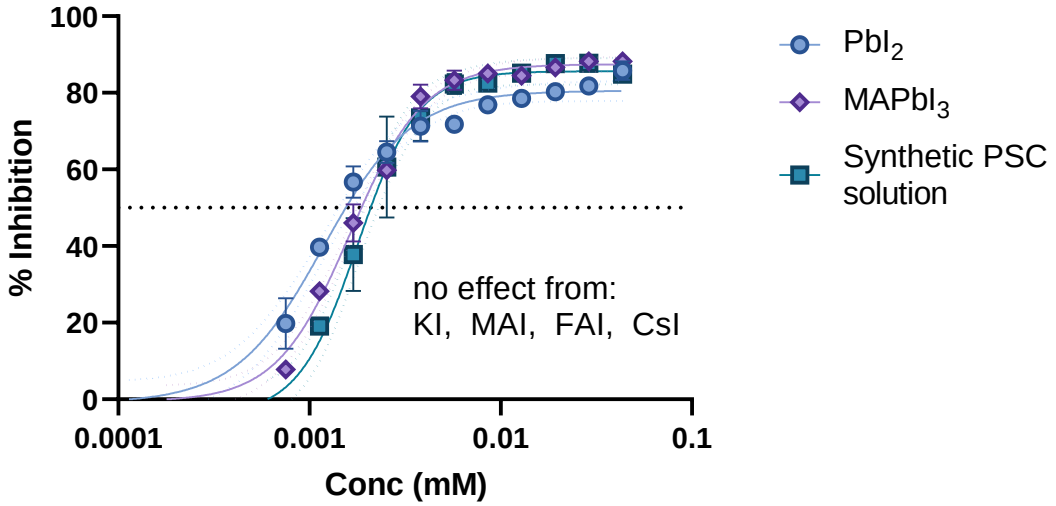

Figure 8: Dose-response curves obtained for toxicity assay using Vibrio fischeri. PbI_2, $MAPbI_3$ and a synthetic PSC solution based on Al / spiro-OMeTAD / $MAPbI_3$ / SnO_2 / ITO were compared. Error bars refer to duplicate measurements.

3. Leaching kinetics: prediction and validation

3.1 Novel analytical approaches to assess leaching kinetics in PSCs

Leaching kinetics are routinely assessed based on standardized protocols to simulate different environmental regimes (e.g. those in solid waste landfills or solid waste exposed to acidic rain). Leaching protocols define an extraction fluid (typically water or mild acid) and a single endpoint (typically after 18-24 hours)[22,23]. However, such protocols do not give time-resolved information and are limited to fast (i.e. < test time) leaching materials. Leaching kinetics will determine the relative concentrations (i.e. mass / volume) of metals in solution and thus strongly influence risk mitigation strategies. In the case of very rapid and quantitative release of Pb^{2+}, improvements in encapsulation or advancements to

The PerTPV project has received funding from the European Union's Horizon 2020 research and innovation programme under grant agreement No 763977.

introduce Pb-scavenging layers within the PSC seem necessary to avoid uncontrolled release[24,25]. In the case of slower leaching kinetics, replacement of the damaged PSC and appropriate end-of-life management might be sufficient[26,27].
Therefore, we established a novel analytical tool to address metal leaching from PSCs on a smaller scale (micro-damage) and with time-resolved data. The system is based on image analysis (to monitor perovskite degradation) and trace metal analytics (to monitor metal leaching) (Figure 9). Setup dimensions allow for the assessment of PSCs of different size and includes typical sizes for lab-scale PSCs (3x3 cm^2). Extraction fluid volume was optimized to minimize unnecessary dilution, while still enabling multiple sampling time points. The setup allows for the detection of Pb differences of 0.45 $\mu g/cm^2$ (or 0.1 % for 3x3 cm^2 cells). A suite of parameters (encapsulation methods, extraction fluid pH and composition, temperature) can be envisioned for testing with this setup and can provide novel insights concerning environmental risk assessment.

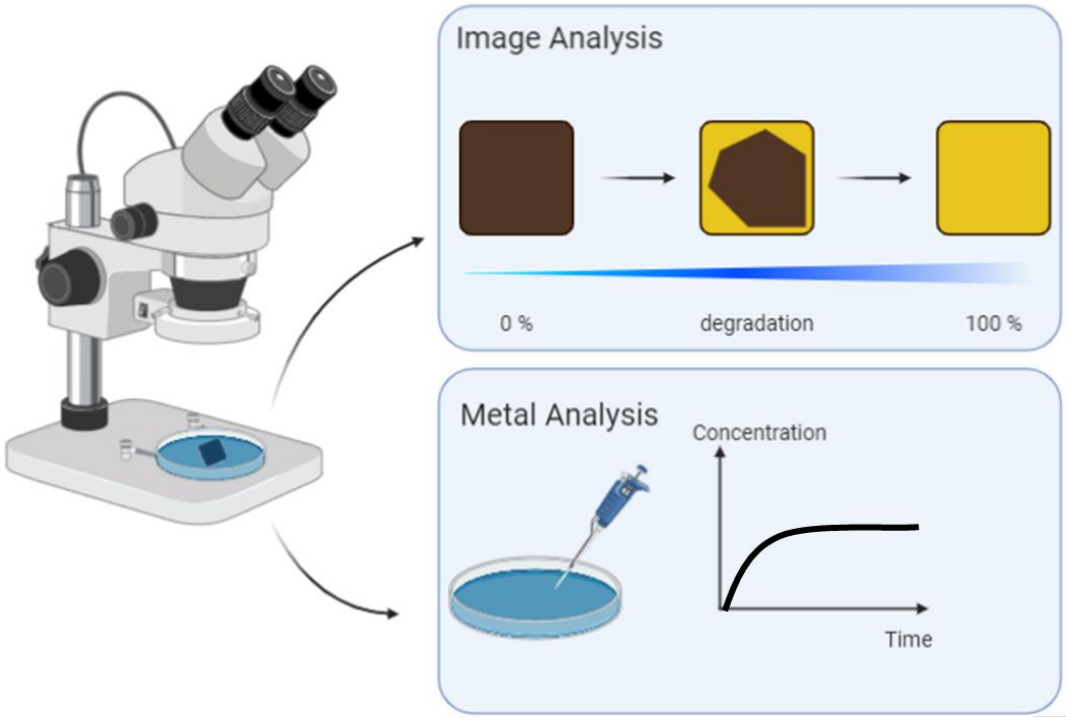

Figure 9: Graphical representation of developed setup to assess leaching kinetics. Image analysis via camera-fitted microscope can be carried out to investigate degradation kinetics. Sampling of the extraction fluid can give temporal information of metal release via ICP-MS.

A proof-of-concept experiment was carried out using minimally encapsulated (plastic-foil without edge-sealing) PSCs in deionised water. Total Pb^{2+} leached over 100 hours accounted to only 17 % (Figure 10 A). Similarly, a leaching rate can also be visualised over time (Figure 10 B). Visual degradation (brown to yellow) was complete, an example picture for image analysis showed good contrast between perovskite phase (brown), PbI_2 phase (yellow) and potentially leached area (transparent) (similar than Figure 10 C). Using this set-up, in the future laser-ablation may be used to introduce defined defects (e.g. pin hole of a certain diameter; a line of a defined width) (Figure 10C) and geometric models for PSC leaching can be derived.

The PerTPV project has received funding from the European Union's Horizon 2020 research and innovation programme under grant agreement No 763977.

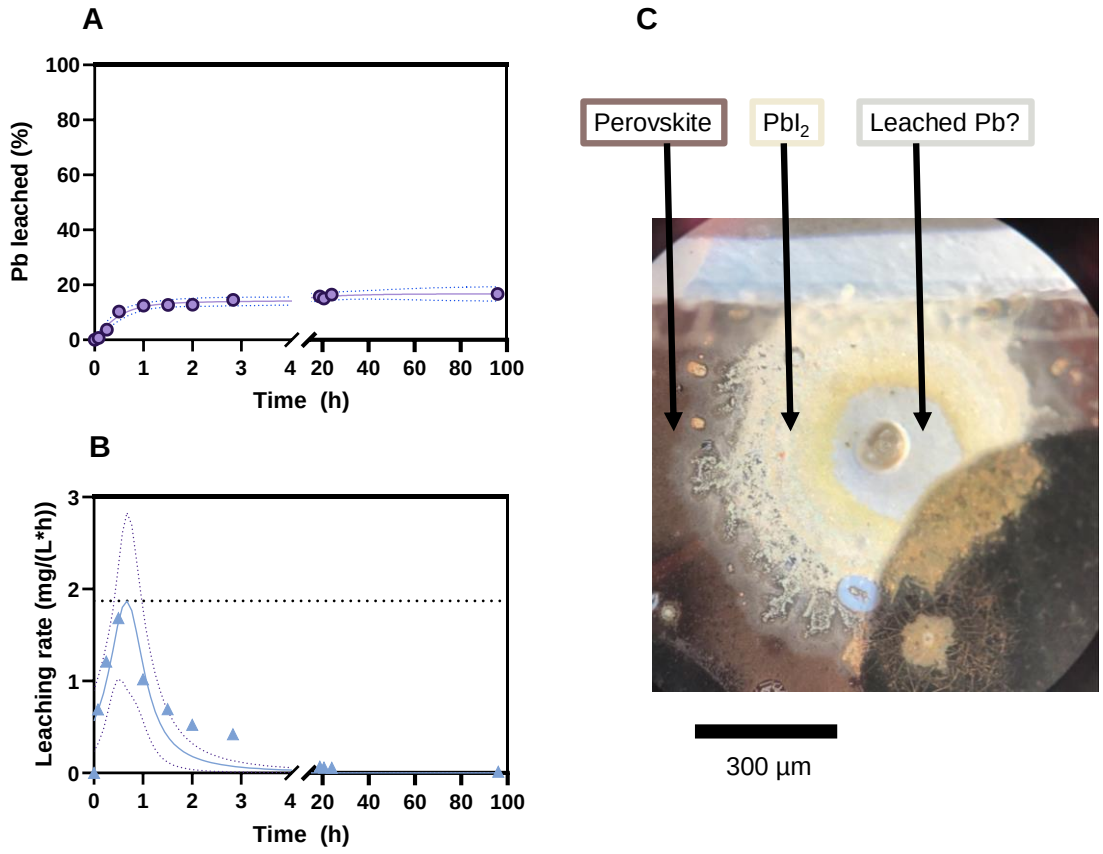

Figure 10: Leaching kinetics tested for a minimally encapsulated PSC. Temporal resolution of leached Pb (A) and leaching rate extrapolation (B) are possible. Appropriate contrast between the different phases (C) allow for image analysis to obtain degradation kinetics data.

3.2 Prediction of environmental concentrations and implications

The worst-case scenario as simulated in the microcosms considered immediate and full dissolution of perovskite-based absorber materials into the aqueous phase at elevated concentrations. Initial leaching kinetics experiments indicated that in a more realistic damage scenario (e.g. moisture ingress via edges), only 17 % of total Pb were leached. Considering PSC area (9 cm^2) and exposure time (100 h), a predicted environmental concentration (PEC) of 0.85 mg Pb m^{-2} h^{-1} was calculated. For a more complex assessment, scenarios based on different exposure pathways should be included. Two main scenarios can be imagined to predict environmental concentrations.

First, in a "solar park-type" assessment, one may imagine a damaged module from which Pb/Sn is leached by rain dripping on the soil below the module. Then, sorption will determine the fraction of bioavailable Pb remaining. More specifically, one may assume complete (100% of 0.5 g Pb m^{-2}) Pb^{2+} leaching from a PSC module (1.64m×1m) into a narrow soil segment (e.g. 10 cm) along the module width. Based on a given soil density (e.g. 1500 kg/m^3) and depth (e.g. 2.5 and 25 cm) a "Pb^{2+} concentration factor" (i.e. a factor 2 = doubling of the Pb concentration) can be derived. For the solar park scenario, a Pb^{2+} concentration factor of 8.8 and 1.8 was obtained for soil depths of 2.5 cm and 25 cm, respectively. Soil concentrations are thus increased by 133 mg/kg and 13 mg/kg. Relating this to the findings from the microcosm experiments, given an exposure of 24 hours, sequestration of Pb^{2+} via sorption will have occurred and limited the extent of potentially available Pb^{2+}. Fractionation from sequential extraction indicated that 37 – 52 % of spiked Pb^{2+} could be potentially liberated, which decreases the most problematic Pb^{2+} fraction to 49.2-69.2 mg/kg (soil depth 2.5 cm) and 4.9-6.9 mg/kg (soil depth 25

The PerTPV project has received funding from the European Union's Horizon 2020 research and innovation programme under grant agreement No 763977.

cm). This is comparable to assumptions made by Hailgenaw et al[28] and does not represent a critical increase in soil Pb concentration. Exchangeable fractions in microcosms ranged from 3.8-8.1 %. Therefore, potentially bioavailable Pb amounts to 5.0-10.8 mg/kg (soil depth 2.5 cm) and 0.5-1.0 mg/kg (soil depth 25 cm). This concentration increase is minimal and below critical toxicity values for soil organisms (e.g. *Folsomia candida* (springtail): LC_{50} = 2562 mg/kg and EC_{50} (reproduction) = 1244 mg/kg[29] or *Eisenia fetida* (earth worm): EC_{50} (reproduction) = 35-5080 mg/kg[30]).

Secondly, in a "rooftop" scenario one may consider as well complete Pb/Sn release from the same module within a single rain event (100 mm as a one-day maximum in Switzerland), which is collected by a downpipe. If the rainwater is directly percolated on to soil, similar concentration factors can be derived as for the solar park scenario. However, if one considers that rain is transferred into either the sewer, a percolation tank or an infiltration pond, maximal aqueous Pb^{2+} concentration should be considered due to the absence of Pb scavenging soil phases. In the rooftop scenario, one can consider a fully covered roof with 50 m^2 of PSCs (with 0.5 g Pb / m^2). As a worst-case, full leaching of Pb^{2+} in a single rain event (100 mm = L/m^2) is assumed. The resultant Pb concentration in the aqueous phase equates to 5 mg/L (25 g of Pb from PSC diluted in 5000 L of rain). This value is identical to the legislative limit for hazardous waste (based on the US resource conservation and recovery act[23]). The concentration exceeds critical toxicity levels for some aquatic organisms (e.g. EC_{50} (mobilization, *daphnia magna*) = 695 µg/L[31]), while being at sub-toxic levels for others (e.g. EC_{50} (malformation, *danio rerio*) = 48 mg/L[20]). EU drinking water limits for Pb are defined at levels of 10 µg/L, so that a 500-fold dilution would be necessary to reach sub-critical limits. It should be noted that here an absolute worst case scenario (50 m^2 of PSC leaching immediately) is considered, which is extremely improbable. Rather, one can assume a minor damage, for instance 0.1 m^2 of PSC leaching after local hail impact. This would result in a Pb concentration of 10 µg/L, only. Indeed, as demonstrated below (see section 3.3), even when physically damaged, PSCs tested did not release major proportions of Pb, confirming that worse case assumptions are in all likely events far too conservative.

3.3 Leaching under natural conditions

When exposed to natural weather conditions, PSC modules are subjected to various destructive factors (UV light, temperature changes, moisture). Their combination can lead to the potential release of harmful PSC components during use or at the end-of-life[32]. Long-term, outdoor leaching studies were carried out using a custom-built outdoor leaching installation (Figure 11). The installation was constructed with stainless steel bars and mounts for the PSC samples. The samples were centred using magnets. The mounts were tilted in order to ensure proper rain runoff through a drain adapter. Rainwater collection occurred after a given rain event, logging the total volume and taking a 10 mL aliquot. The aliquot was filtered to remove biomass and dirt (0.45 µm) and acidified to 3 % HNO_3 prior to ICP-MS analysis.

The PerTPV project has received funding from the European Union's Horizon 2020 research and innovation programme under grant agreement No 763977.

Figure 11: Image of constructed outdoor installation. Stainless steel mounts were constructed to place the PSCs and include a drain for the collection of rainwater.

Metal release from various PSC modules was monitored using ICP-MS after rain and over the course of 11 months. Leaching rates were used to calculate predicted environmental concentrations (PECs) as a basis for environmental exposure risk. Three types of PSCs were mounted and assessed over the course of >150 days. Glass substrate PSCs (received from UOXF, glass / FTO / poly-TPD / $FA_{0.83}Cs_{0.17}Pb(I_{0.9}Br_{0.1})_3$ / PCBM / BCP / Cr / Au, 3x3 cm^2 each) were minimally encapsulated using an EVA plastic foil and hot-melt edge-sealing. PET substrate PSCs (received from VTT, PET / ITO / SnO_2 / $MAPbI_3$ / spiro-OMeTAD / Ag), 10x3 cm^2 each) were fully laminated and mounted as received. Lastly, large-area PSCs (received from UOXF, Glass / FTO / PEDOT:PSS / $FA_{0.83}Cs_{0.17}Pb_{0.5}Sn_{0.5}I_3$ / PCBM / BCP / ITO / PolyTPD / $FA_{0.83}Cs_{0.17}Pb(I_{0.6}Br_{0.4})_3$ / PCBM / BCP / ITO , 11.2x11.2 cm^2) included full encapsulation from Oxford PV (lamination foil and butyl rubber edge seal). Six total large-area samples were received. Two included the full all-perovskite tandem material stack; two included all layers of the tandem EXCEPT the Pb-containing perovskite layers and two blanks. Rainwater was collected after a given rain events and metal concentrations were measured using ICP-MS. Based on this data, cumulative Pb^{2+} leaching was assessed (Table 2). This represents an assessment for the “rooftop” scenario considered in section 3.2, where leached metals would be collected in a sewer. Other metals (In, Sn, Cr, Au, Ag) were monitored during the initial exposure times but were not detectable (< 1 µg / L).

Large-area glass substrate cells were subjected to hail impacted testing after 180 and 243 days. For this, four 30 (40) mm ice balls were fired centrally onto the samples before re-mounting. Predicted environmental concentrations (PECs) were then extracted by including i) PV area ii) rain volume and iii) exposure time.

The PerTPV project has received funding from the European Union’s Horizon 2020 research and innovation programme under grant agreement No 763977.

Table 2: Cumulative Pb levels monitored over 7 and 11 months in rainwater. Measured ICP-MS concentrations were converted into % relative to the maximal expected Pb content.

	Cumulative Pb mobilised (% relative to total amount)			
PSC / Month	glass, minimal encapsulation	PET, encapsulation	PET, encapsulation, damaged	Rainfall (mL, cumulative)
May	0.20	0	0.013	510
June	0.48	0.002	0.015	622
July	2.84	0.021	0.046	1485
August	2.92	0.023	0.046	1705
September	3.85	0.029	0.049	2285
October	4.34	0.033	0.053	2643
November	5.29	0.036	0.056	3344
PSC / Month	All-perovskite tandem	Pb-free tandem	Blank	Rainfall (L, cumulative)
May	0.052	0.028	0.12	2.5
June	0.055	0.028	0.12	3.0
July	0.090	0.029	0.12	4.5
August	0.11	0.035	0.12	5.4
September	0.11	0.042	0.13	6.1
October	0.12	0.054	0.13	8.0
November	0.13	0.059	0.13	8.5
Hail impact testing, 4x 30 mm ice balls per cell at 25-28 m/s				
December	0.14	0.064	0.13	9.4
January	0.15	0.072	0.13	9.9
Hail impact testing, 4x 40 mm ice balls per cell at 25-28 m/s				
February	0.151	0.074	0.13	12.0

Maximal Pb leaching was observed for minimally encapsulated samples. Visual degradation of the perovskite phase (brown to yellow transition) was observed overnight. However, Pb^{2+} leaching of minimally encapsulated PSCs over 7 months equated to only 5.3 ± 1.0 % of total Pb content (determined after 8-month exposure by microwave-assisted acid digestion). Encapsulated cells showed no significant Pb release over the course of the exposure time. For large-area cells, results were similar: proper encapsulation ensured a minimal release of 0.15 ± 0.04 % of total Pb over the tested


The PerTPV project has received funding from the European Union's Horizon 2020 research and innovation programme under grant agreement No 763977.

timeframe. Hail impact of 30 mm (November 2020, Table 2) did not increase metal leaching and emissions. Hail impact of 40 mm (February 2021, Table 2) lead to visual deterioration (and likely loss of function, Figure 12), but Pb release was still marginal, which allows an operator to replace damaged cells after hail and function loss. For the calculation of PEC, total Pb leached in the given area was extrapolated to i) 1 m^2 by adjusting the total PV area ii) 1 year of exposure based on rainfall encountered during the exposition time. For all-perovskite tandem samples, the PEC was calculated to be 0.059 ± 0.016 µg Pb m^{-2} y^{-1}. This is considerably lower compared to the most conservative legislative limits (e.g. 10 µg/L EU drinking water limit).

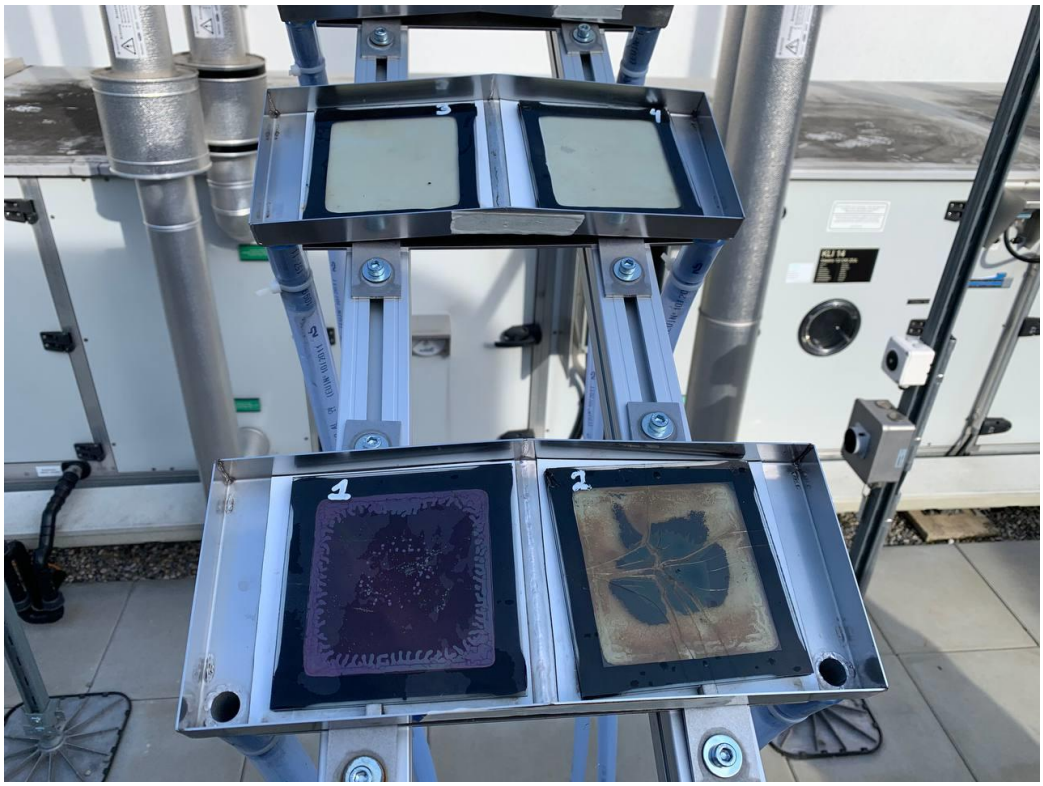

Figure 12: Example picture of large-area all-perovskite tandem cells on the outdoor installation after 40 mm hail impact testing. Cells 1 and 2 (bottom) contain all layers and visual degradation of cell 2 after hail impact is well visible. Cells 3 and 4 (top) included all layers except Pb-based perovskite and were not visually impaired after hail impact testing.

Therefore, encapsulation likely plays a critical role in mitigating potential risks from metal leaching in damage scenarios. Various studies have been carried out to optimize encapsulation and/or even including Pb-sequestering layers[24,25].

All in all, here, we evaluated metal leaching from PSCs under natural weather conditions for the first time and show that i) device encapsulation plays a key role in limiting metal release ii) hail impact does not significantly increase metal emissions and iii) damage scenarios should of course be avoided, but cannot be considered catastrophic .

4. Conclusions

In all microcosm conditions tested, a half-life of Pb^{2+} in the aqueous phase of 0.1-0.9 h was observed and the Pb^{2+} removal after 24 hours ranged between 91 and 98 %. The experiments covered oxidizing to strongly reducing redox conditions, thus were representative for many environments. The rapid and efficient removal was observed despite the applied worst-case scenario where all Pb^{2+} is released immediately to soil. The measured temporal decrease in metal concentration in the presence of sorbents

The PerTPV project has received funding from the European Union's Horizon 2020 research and innovation programme under grant agreement No 763977.

affected metal availability within a few hours. The independence of rapid Pb^{2+} removal kinetics upon the conditions applied, indicated that Pb^{2+} removal from the aqueous phase was mainly driven by physical and not biological processes during initial (< 24 h) exposure. Sorption of soluble Pb^{2+} to the matrix was observed to a high extent and therefore little Pb^{2+} mobility is to be expected in either of the mentioned scenarios. Hence, Pb^{2+} release (and toxicity) was naturally scavenged by sorption to sub-toxic levels. Fate assessment of both the aqueous and soil compartments revealed no considerable differences between perovskite and 'normal' Pb^{2+} contamination. Sorption to mineral phases was found as a potential natural immobilization mechanism confirmed by sequential extraction and X-ray absorption measurements. However, long-term (many months to years) stability and bioavailability of mobile Pb^{2+} fractions (exchangeable and reducible) have not been tested. Even though a considerable amount of Pb^{2+} was removed naturally, the stability and potential transformations liberating Pb^{2+} in the long-term are to this point unknown and would require field assessment. Microcosms spiked with Sn demonstrated similar aqueous removal, but exhibited even stronger immobilisation. The transformation into organotin species was not observed via GC-MS. Mixture toxicity was assessed via a bioluminescence assay and indicated Pb^{2+} levels determine toxicity in a perovskite leachate solution.
A novel analytical approach was developed to address PSC metal leaching and calculate predicted environmental concentrations. Furthermore, 7-month outdoor exposure of minimally encapsulated PSCs resulted in (non-quantitative) release of only 5% of the Pb present in the PSCs. Fully encapsulated cells demonstrated minimal Pb leaching and were able to withstand hail impact testing without substantial increase in metal concentration. From hail-damaged cells left in the field, which present visible cracks in the glass substrates, a predicted environmental concentration of 0.059 ± 0.016 µg Pb m^{-2} y^{-1} was extrapolated. This is notably significantly below permissible levels under any conceivable scenario.

References

(1) Maranghi, S.; Parisi, M. L.; Basosi, R.; Sinicropi, A. Environmental Profile of the Manufacturing Process of Perovskite Photovoltaics: Harmonization of Life Cycle Assessment Studies. *Energies* **2019**, *12* (19), 3746.

(2) Celik, I.; Song, Z.; Phillips, A. B.; Heben, M. J.; Apul, D. Life Cycle Analysis of Metals in Emerging Photovoltaic (PV) Technologies: A Modeling Approach to Estimate Use Phase Leaching. *J. Clean. Prod.* **2018**, *186*, 632–639.

(3) Schileo, G.; Grancini, G. Lead or No Lead? Availability, Toxicity, Sustainability and Environmental Impact of Lead-Free Perovskite Solar Cells. *J. Mater. Chem. C* **2021**.

(4) Hailegnaw, B.; Kirmayer, S.; Edri, E.; Hodes, G.; Cahen, D. Rain on Methylammonium Lead Iodide Based Perovskites: Possible Environmental Effects of Perovskite Solar Cells. *J. Phys. Chem. Lett.* **2015**, *6* (9), 1543–1547.

(5) Li, J.; Cao, H.-L.; Jiao, W.-B.; Wang, Q.; Wei, M.; Cantone, I.; Lü, J.; Abate, A. Biological Impact of Lead from Halide Perovskites Reveals the Risk of Introducing a Safe Threshold. *Nat. Commun.* **2020**, *11* (1), 1–5.

(6) Pietri, J. C. A.; Brookes, P. C. Relationships between Soil PH and Microbial Properties in a UK Arable Soil. *Soil Biol. Biochem.* **2008**, *40* (7), 1856–1861.

(7) Kowalchuk, G. A.; Stephen, J. R. Ammonia-Oxidizing Bacteria: A Model for Molecular Microbial Ecology. *Annu. Rev. Microbiol.* **2001**, *55* (1), 485–529.

(8) Schippers, A. Biogeochemistry of Metal Sulfide Oxidation in Mining Environments,

The PerTPV project has received funding from the European Union's Horizon 2020 research and innovation programme under grant agreement No 763977.

Sediments, and Soils. *Spec. Pap. Soc. Am.* **2004**, 49–62.
(9) Wei, H.; Liu, Y.; Xiang, H.; Zhang, J.; Li, S.; Yang, J. Soil PH Responses to Simulated Acid Rain Leaching in Three Agricultural Soils. *Sustainability* **2020**, *12* (1), 280.
(10) Borch, T.; Kretzschmar, R.; Kappler, A.; Cappellen, P. Van; Ginder-Vogel, M.; Voegelin, A.; Campbell, K. Biogeochemical Redox Processes and Their Impact on Contaminant Dynamics. *Environ. Sci. \& Technol.* **2010**, *44* (1), 15–23.
(11) Kappler, A.; Bryce, C.; Mansor, M.; Lueder, U.; Byrne, J. M.; Swanner, E. D. An Evolving View on Biogeochemical Cycling of Iron. *Nat. Rev. Microbiol.* **2021**, 1–15.
(12) Kwon, K. D.; Refson, K.; Sposito, G. Surface Complexation of Pb (II) by Hexagonal Birnessite Nanoparticles. *Geochim. Cosmochim. Acta* **2010**, *74* (23), 6731–6740.
(13) Baramov, T.; Keijzer, K.; Irran, E.; Mösker, E.; Baik, M.-H.; Süssmuth, R. Synthesis and Structural Characterization of Hexacoordinate Silicon, Germanium, and Titanium Complexes of the E. Coli Siderophore Enterobactin. *Chem. – A Eur. J.* **2013**, *19* (32), 10536–10542. https://doi.org/10.1002/chem.201301825.
(14) Lee, S.; An, J.; Kim, Y.-J.; Nam, K. Binding Strength-Associated Toxicity Reduction by Birnessite and Hydroxyapatite in Pb and Cd Contaminated Sediments. *J. Hazard. Mater.* **2011**, *186* (2–3), 2117–2122.
(15) Jokar, E.; Chien, C.-H.; Tsai, C.-M.; Fathi, A.; Diau, E. W.-G. Robust Tin-Based Perovskite Solar Cells with Hybrid Organic Cations to Attain Efficiency Approaching 10%. *Adv. Mater.* **2019**, *31* (2), 1804835.
(16) Nishimura, K.; Kamarudin, M. A.; Hirotani, D.; Hamada, K.; Shen, Q.; Iikubo, S.; Minemoto, T.; Yoshino, K.; Hayase, S. Lead-Free Tin-Halide Perovskite Solar Cells with 13% Efficiency. *Nano Energy* **2020**, 104858.
(17) Hoch, M. Organotin Compounds in the Environment—an Overview. *Appl. geochemistry* **2001**, *16* (7–8), 719–743.
(18) Kotake, Y. Molecular Mechanisms of Environmental Organotin Toxicity in Mammals. *Biol. Pharm. Bull.* **2012**, *35* (11), 1876–1880.
(19) Ke, W.; Kanatzidis, M. G. Prospects for Low-Toxicity Lead-Free Perovskite Solar Cells. *Nat. Commun.* **2019**, *10* (1), 965.
(20) Babayigit, A.; Ethirajan, A.; Muller, M.; Conings, B. Toxicity of Organometal Halide Perovskite Solar Cells. *Nat. Mater.* **2016**.
(21) Wang, G.; Zhai, Y.; Zhang, S.; Diomede, L.; Bigini, P.; Romeo, M.; Cambier, S.; Contal, S.; Nguyen, N. H. A.; Rosická, P.; others. An Across-Species Comparison of the Sensitivity of Different Organisms to Pb-Based Perovskites Used in Solar Cells. *Sci. Total Environ.* **2020**, *708*, 135134.
(22) Panthi, G.; Bajagain, R.; An, Y.-J.; Jeong, S.-W. Leaching Potential of Chemical Species from Real Perovskite and Silicon Solar Cells. *Process Saf. Environ. Prot. 149*, 115–122.
(23) Moody, N.; Sesena, S.; deQuilettes, D. W.; Dou, B. D.; Swartwout, R.; Buchman, J. T.; Johnson, A.; Eze, U.; Brenes, R.; Johnston, M.; others. Assessing the Regulatory Requirements of Lead-Based Perovskite Photovoltaics. *Joule* **2020**.
(24) Huckaba, A. J.; Sun, D. T.; Sutanto, A. A.; Mensi, M.; Zhang, Y.; Queen, W. L.; Nazeeruddin, M. K. Lead Sequestration from Perovskite Solar Cells Using a Metal--Organic Framework Polymer Composite. *Energy Technol.* **2020**, *8* (7), 2000239.
(25) Li, X.; Zhang, F.; He, H.; Berry, J. J.; Zhu, K.; Xu, T. On-Device Lead Sequestration for Perovskite Solar Cells. *Nature* **2020**, *578* (7796), 555–558.
(26) Binek, A.; Petrus, M. L.; Huber, N.; Bristow, H.; Hu, Y.; Bein, T.; Docampo, P. Recycling Perovskite Solar Cells to Avoid Lead Waste. *ACS Appl. Mater. Interfaces* **2016**, *8* (20), 12881–12886. https://doi.org/10.1021/acsami.6b03767.
(27) Park, S. Y.; Park, J.-S.; Kim, B. J.; Lee, H.; Walsh, A.; Zhu, K.; Kim, D. H.; Jung, H. S. Sustainable Lead Management in Halide Perovskite Solar Cells. *Nat. Sustain.* **2020**, *3* (12), 1044–1051.

The PerTPV project has received funding from the European Union's Horizon 2020 research and innovation programme under grant agreement No 763977.

(28) Hailegnaw, B.; Kirmayer, S.; Edri, E.; Hodes, G.; Cahen, D. Rain on Methylammonium Lead Iodide Based Perovskites: Possible Environmental Effects of Perovskite Solar Cells. *J. Phys. Chem. Lett.* **2015**, *6* (9), 1543–1547.
(29) Dai, W.; Holmstrup, M.; Slotsbo, S.; Ke, X.; Li, Z.; Gao, M.; Wu, L. Compartmentation and Effects of Lead (Pb) in the Collembolan, Folsomia Candida. *Environ. Sci. Pollut. Res.* **2020**, *27* (35), 43638–43645.
(30) Lanno, R. P.; Oorts, K.; Smolders, E.; Albanese, K.; Chowdhury, M. J. Effects of Soil Properties on the Toxicity and Bioaccumulation of Lead in Soil Invertebrates. *Environ. Toxicol. Chem.* **2019**, *38* (7), 1486–1494.
(31) Kim, H.; Yim, B.; Bae, C.; Lee, Y.-M. Acute Toxicity and Antioxidant Responses in the Water Flea Daphnia Magna to Xenobiotics (Cadmium, Lead, Mercury, Bisphenol A, and 4-Nonylphenol). *Toxicol. Environ. Health Sci.* **2017**, *9* (1), 41–49.
(32) Schmidt, F.; Zimmermann, Y.-S.; dos Reis Benatto, G. A.; Kolvenbach, B. A.; Schäffer, A.; Krebs, F. C.; van Hullebusch, E. D.; Lenz, M. Biodeterioration Affecting Efficiency and Lifetime of Plastic-Based Photovoltaics. *Joule* **2020**.

The PerTPV project has received funding from the European Union's Horizon 2020 research and innovation programme under grant agreement No 763977.